

The set-up of a high temperature superconductor radio-frequency SQUID microscope for magnetic nanoparticle detection

To cite this article: M Schmidt *et al* 2006 *Supercond. Sci. Technol.* **19** S261

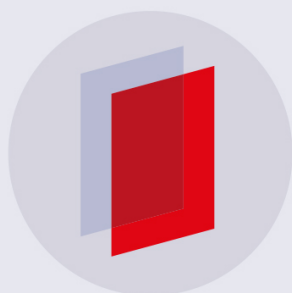
View the [article online](#) for updates and enhancements.

Related content

- [High temperature superconductor dc-SQUID microscope with a soft magnetic fluxguide](#)
U Poppe, M I Faley, E Zimmermann *et al.*
- [High temperature superconductor dc SQUID micro-susceptometer for room temperature objects](#)
M I Faley, K Pratt, R Reineman *et al.*
- [Topical review](#)
Vittorio Pizzella, Stefania Della Penna, Cosimo Del Gratta *et al.*

Recent citations

- [Crystallization Of Glass-Ceramic Bi3Sr2Ca2Cu3Oy Superconducting System](#)
O. Kizilaslan and M.A. Aksan
- [Integrated High-Temperature Superconductor Radio-Frequency Superconducting Quantum Interference Device Covered with Superconducting Thin Films in Flip-Chip Configuration](#)
Yoshimi Hatsukade *et al*
- [The single crystal superconducting Bi-2212 whiskers fabrication and their thermal transport properties](#)
S. Altn *et al*



IOP | ebooks™

Bringing you innovative digital publishing with leading voices to create your essential collection of books in STEM research.

Start exploring the collection - download the first chapter of every title for free.

The set-up of a high temperature superconductor radio-frequency SQUID microscope for magnetic nanoparticle detection

M Schmidt^{1,2}, H-J Krause¹, M Banzet¹, D Lomparski¹, J Schubert¹,
W Zander¹, Y Zhang¹, R Akram³ and M Fardmanesh^{3,4}

¹ Institute of Thin Films and Interfaces, Forschungszentrum Jülich, 52425 Jülich, Germany

² Biotechnological Biomedical Centre, University of Leipzig, Deutscher Platz 5,
04103 Leipzig, Germany

³ Electrical and Electronics Engineering Department, Bilkent University, 06800 Bilkent,
Ankara, Turkey

⁴ Electrical Engineering Department, Sharif University of Technology, Tehran, Iran

E-mail: h.-j.krause@fz-juelich.de

Received 1 September 2005, in final form 27 October 2005

Published 6 March 2006

Online at stacks.iop.org/SUST/19/S261

Abstract

SQUID (superconducting quantum interference device) microscopes are versatile instruments for biosensing applications, in particular for magnetic nanoparticle detection in immunoassay experiments. We are developing a SQUID microscope based on an HTS rf SQUID magnetometer sensor with a substrate resonator. For the cryogenic set-up, a configuration was realized in which the cryostat is continuously refilled and kept at a constant liquid nitrogen level by an isolated tube connection to a large liquid nitrogen reservoir. The SQUID is mounted on top of a sapphire finger, connected to the inner vessel of the stainless steel cryostat. The vacuum gap between the cold SQUID and room temperature sample is adjusted by the precise approach of a 50 μm thin sapphire window using a single fine thread wheel. We investigated possible sensing tip configurations and different sensor integration techniques in order to achieve an optimized design. A new scheme of coupling the rf SQUID from its back to a SrTiO_3 substrate resonator was adopted for the purpose of minimization of the sensor-to-sample spacing. By SQUID substrate thinning and washer size reduction, the optimum coupling conditions for back coupling were determined for different rf SQUID magnetometers prepared on LaAlO_3 and SrTiO_3 substrates. The SQUID microscope system is characterized with respect to its spatial resolution and its magnetic field noise. The SQUID microscope instrument will be used for magnetic nanoparticle marker detection.

1. Introduction

SQUID microscopes have proven useful tools for numerous applications in magnetic imaging with high spatial resolution [1, 2]. The use of HTS SQUIDs permits relatively simple cryogenic designs with only a moderate loss in sensitivity as compared to conventional LTS sensors. To our knowledge,

all HTS SQUID microscopes realized thus far are using dc SQUIDs. Utilizing HTS rf SQUIDs, however, allows a purely inductive, non-galvanic readout of SQUIDs with a high field sensitivity in single layer technology. Since our SQUID microscope set-up is aimed for magnetic nanoparticle marker detection and quantification for monitoring biological immunoreactions [3, 4], we need a high magnetic field sensitivity and

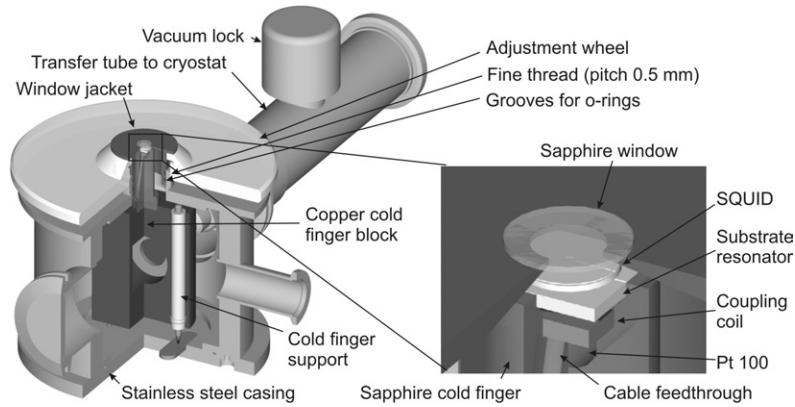


Figure 1. Sketch of the SQUID microscope set-up.

a small spacing between the room temperature sample and cryogenic SQUID. This paper describes the optimization of the HTS rf SQUID for this microscopic application using the substrate resonator scheme [5].

2. Experimental set-up

Our set-up for the HTS rf SQUID microscope is illustrated in figure 1. The casing of the microscope is manufactured from stainless steel and contains a copper cold finger block with a sapphire cold finger mounted on top. A double-walled tube connects the microscope recipient to a liquid nitrogen supply Dewar. By means of a fine thread with a pitch of 0.5 mm, an adjustment wheel made from Plexiglas is connected to the steel flange. A 50 μm thin sapphire window is glued to cover the 8 mm bore of a Vespel jacket carrier which is inserted in the cold finger element using o-ring seals. This ensures vacuum tight vertical mobility of the jacket when the distance between the window and SQUID underneath is altered by rotating the Plexiglas wheel. Rotating the disc by one of the pins distributed around the circumference corresponds to an approach of the window by 3.9 μm . Two cold finger supports with sharp tips ensure minimal thermal losses and allow additional adjustment of the SQUID position below the measurement window.

The coupling coil is affixed in the bottom groove of the sapphire with two-component epoxy glue. In the slot above the coupling coil, the substrate resonator is inserted. The substrate resonator is fixed only using silicone grease because it might need to be changed. The SQUID is also fixed with a very thin layer of silicone grease.

3. RF SQUID optimization

3.1. Washer size and effective area

The washer size of a standard SQUID (diameter 3.5 mm) is too large for SQUID microscopy since it requires too large a window diameter and thus a thick window. Therefore, the effect of size reduction of the SQUID washer was examined. The effective area, the reciprocal of the field-to-flux coefficient, was measured for different SQUID washer diameters (left graph of figure 2). A washer diameter of 2 mm ($A_{\text{washer}} = 1.57 \text{ mm}^2$) turned out to still yield a high effective area and thus

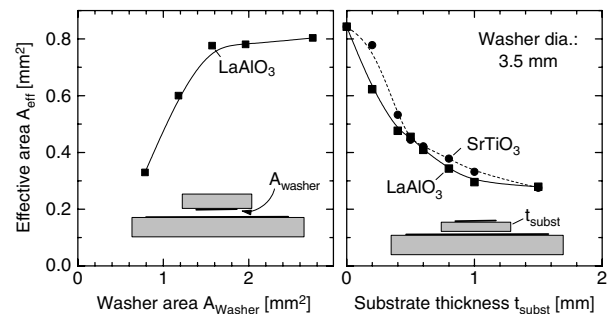


Figure 2. Measured effective area of the SQUID as a function of its washer area (coupled face to face to the substrate resonator) and of the substrate material and thickness (distance to the substrate resonator).

a good sensitivity. For washer diameters below 1.5 mm, the effective area of the magnetometer drops considerably. Thus, it was concluded that a washer diameter of 1.5–2 mm constitutes a good compromise between size reduction and performance.

The standard configuration of coupling an HTS rf SQUID to a substrate resonator is realized by mounting the SQUID chip on the resonator chip in a flip-chip configuration with their superconducting washers face to face [5] (see the left inset in figure 2). For a SQUID microscope, this configuration is unsuitable because the substrate thickness prevents the active SQUID layer from being brought close to the window. Therefore, we need to adopt a new scheme called back coupling (sketched in the right inset in figure 2): the SQUID is flipped such that its active superconducting layer directly faces the window, not the resonator. Thus, the coupling of the SQUID to the resonator has to be performed through the SQUID substrate. We examined the consequences of back coupling for both LaAlO_3 and SrTiO_3 substrates. The measured effective area of the SQUID magnetometer as a function of the substrate thickness is plotted in the right graph of figure 2 for both substrate materials. The value at $t_{\text{subst}} = 0$ was taken in the standard orientation as sketched in the left inset. As expected, the effective area of the sensor drops considerably with increasing distance between active SQUID layer and resonator washer layer, independently of the substrate material.

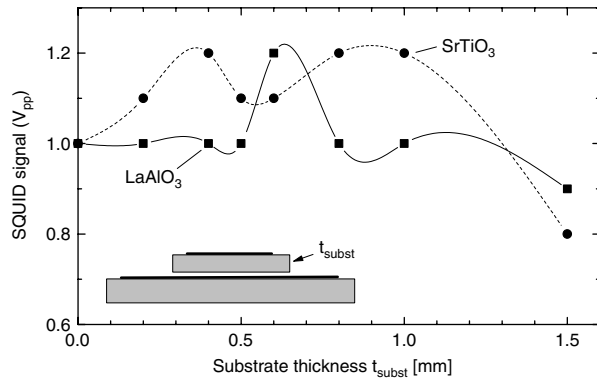


Figure 3. Measured peak-to-peak amplitude of a SQUID, back coupled to a substrate resonator, as a function of the substrate material and thickness.

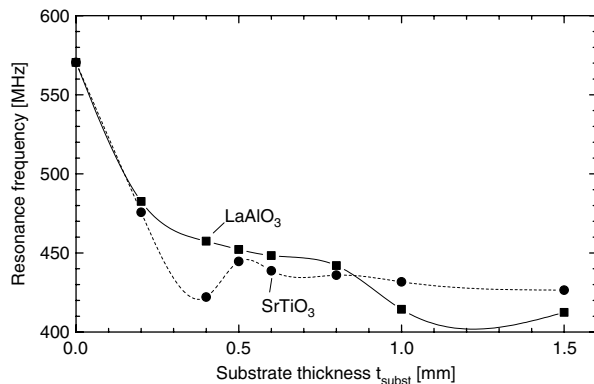


Figure 4. Measured resonance frequency of a substrate resonator with a back coupled SQUID, as a function of the SQUID substrate material and thickness.

3.2. Coupling between the SQUID and substrate resonator

Adopting the scheme of back coupling for rf SQUIDs with the substrate resonator has a number of consequences for SQUID operation. We examined the open-loop peak-to-peak signal amplitude (also called the modulation depth) of the rf SQUID as a function of substrate thickness for both LaAlO₃ and SrTiO₃ substrate material in the configuration of a flipped SQUID with its superconducting side facing away from the resonator, as seen in figure 3. The signal amplitude is given at the output of the SQUID electronics after rf demodulation and amplification by about a factor of 1000. Except for a significant decrease at large substrate thickness observed for both substrate materials, only slight amplitude variations were observed.

Furthermore the dependence of the parameters of the resonance of the substrate resonator-SQUID system was examined as a function of substrate thickness. Figure 4 depicts the measured resonance frequency. Figure 5 displays the experimentally determined quality factor of the resonance.

We note that the resonance frequency decreases steadily with increasing substrate thickness for both substrate materials. The quality factor, however, exhibits a maximum at a substrate thickness of 0.4 mm in both cases. We conclude that the coupling resonance is overdamped in the case of standard

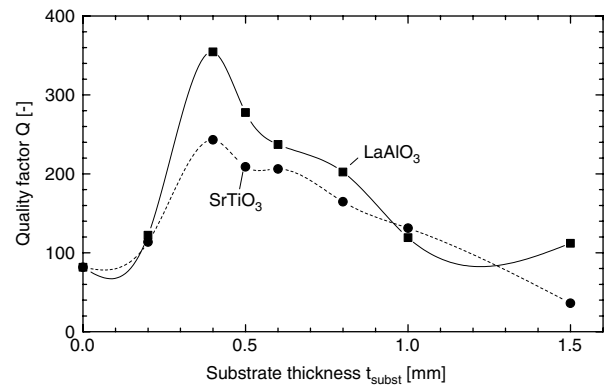


Figure 5. Measured quality factor of a substrate resonator with a back coupled SQUID, as a function of the SQUID substrate material and thickness.

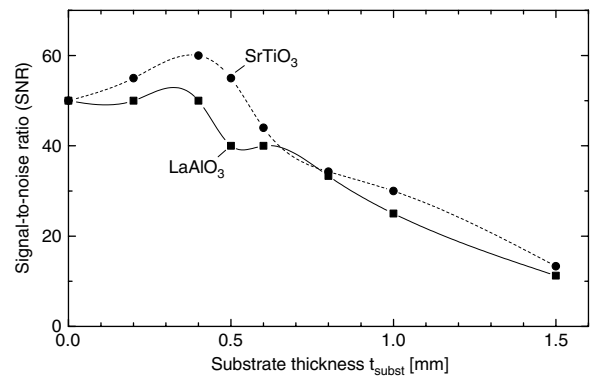


Figure 6. Measured signal-to-noise ratio of a SQUID, back coupled to a substrate resonator, as a function of the substrate material and thickness.

face-to-face coupling and underdamped for large substrate thickness.

The most important factor for determining optimum operation conditions of a back coupled rf SQUID, however, is the ratio of the SQUID signal amplitude to its noise at a constant ambient field. Figure 6 displays this experimentally determined signal-to-noise ratio (SNR) as a function of the SQUID substrate thickness and material.

For both substrate materials, the maximum SNR was found for a thickness around 0.4 mm. This finding is consistent with the measured maxima in the quality factor of the resonance. It was concluded that a suitable rf SQUID configuration should consist of a 1.5 mm washer SQUID on a 0.4 or 0.5 mm substrate, coupled to a substrate resonator from the back. With this configuration, a sensitivity of $13.1 \text{ nT}/\Phi_0$ and a white magnetic field noise of $0.9 \text{ pT Hz}^{-1/2}$ were achieved.

4. Experimental results

4.1. Spatial resolution

The effective magnetic field spatial resolution of the SQUID microscope set-up was determined experimentally by scanning a current-carrying wire (diameter 0.1 mm) across the

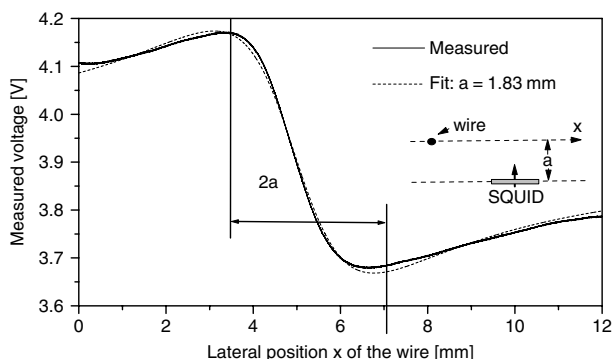


Figure 7. Measurement of the spatial resolution with a 1.5 mm diameter washer SQUID on a 1 mm thick LaAlO₃ substrate, back coupled to a SrTiO₃ substrate resonator. A current-carrying wire was scanned across the microscope head at a distance of approximately 0.2 mm.

measurement window. The wire was stretched between two plastic supports. Care was taken to ensure that the wire is continuously touching the sapphire window while gliding across. The wire support was moved using a micrometer screw driven by a stepper motor. The isolation vacuum distance between the SQUID and window was about 0.1 mm, leading to a total minimum distance $a \approx 200 \mu\text{m}$ between the SQUID and wire.

Figure 7 displays the result of a lock-in measurement of the field of the wire measured with the SQUID during the scanning. From the expression for the magnetic field of a current-carrying wire, $|B(r)| = \frac{\mu_0 I}{2\pi r}$, the vertical magnetic field is derived as $B(x) = \frac{\mu_0 I}{2\pi} \cdot \frac{x}{a^2 + x^2}$ (see the inset of figure 7). The experimental data could be fitted well with this expected behaviour, but with an effective distance $a = 1.83 \text{ mm}$. Thus, the substrate resonator SQUID magnetometer behaves like a point sensor at a distance of 1.83 mm from the source even though the spacing between the active SQUID layer and source is only about 0.2 mm.

This large discrepancy between the small SQUID–sample distance and large effective spatial resolution is attributed to the flux focusing effect of the substrate resonator. Its 10 mm \times 10 mm YBCO washer stands back only 0.5 mm behind the SQUID and focuses the field within a radius of 1.9 mm according to the Ketchen formula [6]. However, as we intend to measure the magnetic moment of a solution containing magnetic nanoparticles in a confined volume (e.g. one well of a 96-well microtitre plate), a small distance in conjunction with a high field sensitivity is more important than spatial resolution. It only has to be ensured that neighbouring volumes do not contribute. With our SQUID–sample distance of $a = 200 \mu\text{m}$ and with an optimized pickup area of $2\pi a^2$, we expect a signal of 500 pT from a large magnetic bead (Dynabead M450 from Dynal, Inc., magnetic moment approximately 10^{-13} A m^2 [7]).

4.2. Magnetic field noise

Figure 8 shows a noise spectrum of the SQUID microscope recorded during operation without the sample and with the vacuum pump switched off. As shown in the figure, the $1/f$ noise dominates below 10 Hz. From 10 to 600 Hz,

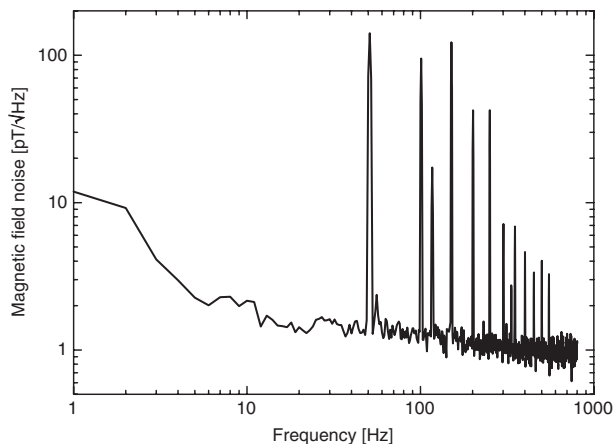


Figure 8. Measured magnetic field noise of the SQUID, back coupled to a substrate resonator, mounted in the SQUID microscope, with the vacuum pump switched off.

discrete disturbance frequencies such as the line frequency and harmonics are observed. When the turbomolecular pump is running, additional vibrational lines at its rotational frequency and harmonics appear. At frequencies above 600 Hz, white noise is predominant. As the magnetic detection of magnetic nanoparticles is usually performed at a single frequency, this measurement frequency should be chosen in a frequency regime where the noise is minimal. Since the frequency regime from 1 to 50 kHz is most relevant for magnetic nanoparticle measurements, one can expect to operate in the regime of intrinsic white SQUID sensor noise.

5. Conclusions and outlook

For the first time, a SQUID microscope based on an HTS rf SQUID magnetometer sensor was realized. The new back coupling scheme was developed in order to achieve an optimum rf SQUID configuration with a substrate resonator which allows minimum distance to the sample at room temperature. We analysed the effective area, the signal amplitude, the resonance frequency, the quality factor and the signal-to-noise ratio of the rf SQUID as a function of the relevant washer and substrate parameters. Thus, the optimum coupling conditions for back coupling were determined for rf SQUID magnetometers prepared on LaAlO₃ and SrTiO₃ substrates. The characterization of the SQUID microscope system proved that a high magnetic field resolution and a close SQUID–sample spacing were indeed achieved, albeit at reduced spatial resolution.

Future work will be directed towards determination of the minimum detectable magnetic moment and, if necessary, an improvement of the spatial resolution. The SQUID microscope instrument will be operated and used in experiments involving magnetic nanoparticles for magnetic immunoassay characterization in the near future. Other intended applications include the investigation of antigen–antibody reactions in fluid samples and DNA detection and hybridization based on the detection of magnetic nanoparticle markers. It is expected that the SQUID microscope will be a

valuable tool in magnetic imaging of biomagnetic samples and will become a prerequisite in magnetic biosensing.

Acknowledgments

This work was supported in part by the German BMBF and the Turkish TUBITAK under Grant 42.6.I3B.2.A and by the German BMWi under Grant 16IN0244.

References

- [1] Kirtley J R and Wikswo J P 2000 Scanning SQUID microscopy *Annu. Rev. Mater. Sci.* **29** 117–48
- [2] Wellstood F C, Matthews J and Chatrathorn S 2003 Ultimate limits to magnetic imaging *IEEE Trans. Appl. Supercond.* **13** 258–60
- [3] Enpuku K, Minotani T, Hotta M and Nakahodo A 2001 Application of high T_c SQUID magnetometer to biological immunoassays *IEEE Trans. Appl. Supercond.* **11** 661–4
- [4] Chemla Y R, Grossman H L, Poon Y, McDermott R, Stevens R, Alper M D and Clarke J 2000 Ultrasensitive magnetic biosensor for homogeneous immunoassay *Proc. Natl Acad. Sci. USA* **97** 14268–72
- [5] Zhang Y, Schubert J, Wolters N, Banzet M, Zander W and Krause H-J 2002 Substrate resonator for HTS rf SQUID operation *Physica C* **372–376** 282–5
- [6] Ketchen M B, Gallagher W J, Kleinsasser A W, Murphy S and Clem J R 1985 The dc SQUID focuser *SQUID '85* ed H D Hahlbohm and H Lübbig (Berlin: de Gruyter) pp 865–71
- [7] Häfeli U, Schütt W, Teller J and Zborowski M 1997 *Scientific and Clinical Applications of Magnetic Carriers* (New York: Plenum)